STABILITY AND ACCURACY OF NUMERICAL BOUNDARY CONDITIONS IN AEROELASTIC ANALYSIS

M. B. GILES

Oxford University Computing Laboratory, Numerical Analysis Group, Wolfson Building, Parks Road, Oxford OX1 3QD, U.K.

SUMMARY

This paper analyses the accuracy and numerical stability of coupling procedures in aeroelastic modelling. A two-dimensional model problem assuming unsteady inviscid flow past an oscillating wall leads to an even simpler one-dimensional model problem. Analysis of different numerical algorithms shows that in general the coupling procedures are numerically stable, but care is required to achieve accuracy when using very few time steps per period of natural oscillation of the structure. The relevance of the analysis to fully three-dimensional applications is discussed. © 1997 by John Wiley & Sons, Ltd.

KEY WORDS: numerical analysis; boundary conditions; aeroelasticity

1. INTRODUCTION

This analysis is motivated by interest in numerical procedures for coupling an unsteady CFD computation to an unsteady structural dynamics model to predict aeroelastic behaviour. Extremely large 3D computations of this sort are necessary to accurately predict the onset of flutter in both turbomachinery and aircraft applications. One approach to the numerical approximation of this problem is the use of a single consistent, fully coupled discretization modelling both the structure and the fluid as a continuum whoss dynamics is governed by partial differential equations, plus boundary conditions at the interfaces. However, for the solid the relevant PDE is the equation of motion for an elastic solid, while for the fluid the appropriate equations are the Navier–Stokes equations with suitable turbulence modelling. Moreover, each has its own characteristic length scales and time scales. Therefore the production of a single fully coupled code for the combined aeroelastic application is at least as much work as writing the individual programmes for the separate solid and fluid applications. Since there are existing codes which accurately and efficiently solve these individual problems, the more practical approach is to investigate how best to couple such codes together to analyse aeroelastic problems.[1–4] One concern is whether the coupling procedure may introduce a spurious numerical instability, unrelated to the real flutter instabilities which are the focus of engineering attention. Another concern is the accuracy of the resulting coupled analysis, particularly when there are very few time steps per period of oscillation.

The general theory for the analysis of numerical interface or boundary condition instabilities is well established but can be complicated to apply in practice.[5–8] In this paper we simplify the analysis by restricting attention to a simple 1D model problem. Section 2 of the paper constructs the model,

explaining its relevance to the real 3D engineering problem. Section 3 considers one particular discretization of the wall dynamics and the fluid dynamics, and a number of different treatments of the coupling between the two. The analysis, and supporting numerical experiments reveal that in general there is no spurious numerical instability, but there can be a problem with the accuracy of the numerical approximation of the solid/fluid coupling. This may lead to a poor approximation of the stability properties of a 3D aeroelastic system. Section 4 presents alternative discretizations of the structural dynamics and associated aerodynamic boundary conditions based on a different form of the structural dynamic equations. The final two sections give some further discussion of the relevance of the analysis to real 3D engineering applications (Section 5) and then draw some conclusions (Section 6).

2. ANALYTIC EQUATIONS

As shown in Figure 1, we start by considering a steady 2D parallel flow with velocity $(0, V)^{\mathrm{T}}$ in the region $x > 0$. The equations describing isentropic linearized perturbations to this compressible 2D flow field are

$$
\frac{\partial}{\partial t}\begin{pmatrix} p \\ u \\ v \end{pmatrix} + \begin{pmatrix} 0 & \rho c^2 & 0 \\ 1/\rho & 0 & 0 \\ 0 & 0 & 0 \end{pmatrix} \frac{\partial}{\partial x}\begin{pmatrix} p \\ u \\ v \end{pmatrix} + \begin{pmatrix} V & 0 & \rho c^2 \\ 0 & V & 0 \\ 1/\rho & 0 & V \end{pmatrix} \frac{\partial}{\partial y}\begin{pmatrix} p \\ u \\ v \end{pmatrix} = 0, \tag{1}
$$

where ρ and c are the average density and speed of sound respectively and p, u and v are the unsteady perturbations to the pressure and the two velocity components respectively.

If the wall oscillates so that its position $x_w(t)$ is independent of y, then the resulting fluid perturbation will also be independent of y, and there will be no perturbation to the velocity in the y-direction. This reduces the linear unsteady aerodynamic equations to the simple form

$$
\frac{\partial}{\partial t}\begin{pmatrix} p \\ u \end{pmatrix} + \begin{pmatrix} 0 & \rho c_2 \\ 1/\rho & 0 \end{pmatrix} \frac{\partial}{\partial x}\begin{pmatrix} p \\ u \end{pmatrix} = 0, \tag{2}
$$

which is the same set of equations as those describing perturbations to a 1D stationary flow with the same density and speed of sound. It is interesting, and perhaps surprising, that these equations do not depend on the Mach number of the mean flow; this is because the assumption of no variation in the y-direction allows a Lagrangian transformation to new co-ordinates $x^* = x$ and $y^* = y - Vt$, relative to which the mean flow is indeed stationary.

Having justified the simple 1D aerodynamic equations, the other aspect of the model formulation is the interaction between the aerodynamics and the motion of the wall. One boundary condition is the linearized kinematic condition that the flow velocity relative to the moving wall is zero:

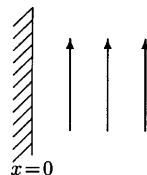$$
\dot{x}_{\mathrm{w}}(t) = u(0, t). \tag{3}
$$

Figure 1. Parallel flow past a flat wall

The dynamics of the wall motion is modelled by a simple mass–spring system subject to the external unsteady aerodynamic pressure:

$$m\ddot{x}_w + m\omega_0^2 x_w = -p(0, t). \tag{4}$$

Here m represents the mass per unit area and ω_0 is the natural frequency of oscillation in the absence of any aerodynamic coupling. This equation will be referred to as the scalar version of the wall dynamic equation. Some numerical discretizations start from an equivalent coupled system of first-order ODEs,

$$\frac{dw}{dt} + Aw = P, \tag{5}$$

where

$$w = \begin{pmatrix} \omega_0 x_w \\ \dot{x}_w \end{pmatrix}, \qquad A = \begin{pmatrix} 0 & -\omega_0 \\ \omega_0 & 0 \end{pmatrix}, \qquad P = \begin{pmatrix} 0 \\ -p(0, t)/m \end{pmatrix}. \tag{6}$$

This will be referred to as the vector version of the equation.

This simple structural model seems far removed from the original representation of a continuum elastic solid discussed in Section 1. In fact, it is common to represent the dynamics of an oscillating blade in terms of a very limited number of structural modes; these are usually obtained using a finite element approximation of the elastic solid vibrating in the absence of any external aerodynamics. The modes with the lowest natural frequency are the ones which have the greatest potential for flutter and large forced excitation, which is why higher modes are neglected. The lowest mode is usually a simple bending mode whose nature is very similar to the simple undamped mass–spring system. Even a torsional mode can be viewed locally (near the blade surface) as being similar to the model problem in that there are no large variations in the tangential direction and so 1D aerodynamics is a good local approximation. In other 2D and 3D computations with numerical instabilities at interfaces it is generally true that any instability will first occur with a purely 1D eigenmode with a spatial variation in the direction normal to the interface but no variation along the interface. Thus the 1D model problem should be appropriate in trying to identify the possibility of a purely numerical instability.

This simple model problem exhibits aerodynamic damping of the wall oscillation. To determine this, it is helpful to perform a change of variables in the aerodynamic equations. Characteristic variables defined by

$$q = p + \rho c u, \qquad r = p - \rho c u \tag{7}$$

satisfy the uncoupled equations

$$\frac{\partial q}{\partial t} + c\frac{\partial q}{\partial x} = 0, \qquad \frac{\partial r}{\partial t} - c\frac{\partial r}{\partial x} = 0. \tag{8}$$

The acoustic wave represented by q travels right with velocity c, while the other acoustic wave represented by r travels left with velocity $-c$. We need to impose a radiation condition at $x = \infty$ requiring that sufficiently far from the wall all perturbations are travelling away from the wall, not towards it. Thus we require that $r \to 0$ as $x \to \infty$.

Using the characteristic variables, the equations for the wall are

$$\dot{x}_w = \frac{1}{2\rho c}[q(0, t) - r(0, t)], \qquad m\ddot{x}_w + m\omega_0^2 x_w = -\tfrac{1}{2}[q(0, t) + r(0, t)]. \tag{9}$$

We now consider solutions of the form

$$x_w(t) = Xe^{i\omega t}, \qquad q(x, t) = Qe^{i\omega(t - x/c)}, \qquad r(x, t) = 0, \tag{10}$$

with X and Q being complex constants. The real physical variables correspond to the real components of these complex expressions. These solutions satisfy the necessary equations and boundary conditions provided that

$$\mathrm{i}\omega X = \frac{1}{2\rho c}Q, \qquad (-m\omega^2 + m\omega_0^2)X = -\tfrac{1}{2}Q, \tag{11}$$

for which non-trivial solutions exist only if

$$-m\omega^2 + \mathrm{i}\omega\rho c + m\omega_0^2 = 0 \quad \Rightarrow \quad \frac{\omega}{\omega_0} = \mathrm{i}d \pm \sqrt{(1-d^2)}, \tag{12}$$

where $d = \rho c/2m\omega_0$ is the non-dimensional damping factor. In real turbomachinery applications modelled using a structure with a single degree of freedom, the level of damping is very small, usually in the range 0·005–0·02. For aircraft applications concerned with wing aeroelasticity, values in the range 0·05–0·2 are more typical. Assuming that d is small,

$$\frac{\omega}{\omega_0} = \mathrm{i}d \pm (1 - \tfrac{1}{2}d^2) + O(d^4). \tag{13}$$

Taking the positive root without any loss of generality (since the real variables correspond to the real component only) gives

$$\mathrm{e}^{\mathrm{i}\omega t} \approx \mathrm{e}^{\mathrm{i}\omega_0 t - d\omega_0 t} \tag{14}$$

and so the fractional reduction in the wall oscillation amplitude in one period of oscillation is

$$1 - \mathrm{e}^{-2\pi d} \approx 2\pi d. \tag{15}$$

The model equations do not have any terms describing energy dissipation. It can be shown that this reduction in the vibrational energy of the wall is in fact exactly equal to the acoustic energy radiated during the period of oscillation.

In considering discretizations of the model equations, one question is whether the discrete approximation allows unstable exponentially growing solutions with a time scale which is much smaller than the period of oscillation $2\pi/\omega_0$. If there is no such instability, then the main question is how accurately the aerodynamic damping is modelled by the discretization.

3. STRUCTURAL ALGORITHMS BASED ONLY ON WALL DISPLACEMENT

In this section we consider coupled aeroelastic discretizations in which the scalar form of the wall dynamic equation is approximated using central time differencing:

$$\frac{m}{\Delta t^2}(x_{\mathrm{w}}^{(n+1)} - 2x_{\mathrm{w}}^{(n)} + x_{\mathrm{w}}^{(n-1)}) + m\omega_0^2 x_{\mathrm{w}}^{(n)} = -\tfrac{1}{2}(q_0^{(n)} + r_0^{(n)}). \tag{16}$$

A number of different discretizations of the kinematic condition will be analysed.

3.1. Upwind aerodynamic discretization

The first algorithms are based on upwind discretization of the aerodynamic equations. Using forward time differencing and upwind spatial differencing, the interior equations are

$$\begin{aligned}
q_j^{(n+1)} &= q_j^{(n)} - \frac{c\Delta t}{\Delta x}(q_j^{(n)} - q_{j-1}^{(n)}), \quad j = 1, 2, 3, \ldots, \\
r_j^{(n+1)} &= r_j^{(n)} + \frac{c\Delta t}{\Delta x}(r_{j+1}^{(n)} - r_j^{(n)}), \quad j = 0, 1, 2, \ldots.
\end{aligned} \tag{17}$$

The stability analysis considers the possible existence of a G–R (Godunov–Ryabenkii) normal mode[5,7] of the form

$$x_{\mathrm{w}}^{(n)} = Xz^n, \qquad q_j^{(n)} = Qz^n\kappa_q^j, \qquad r_j^{(n)} = Rz^n\kappa_r^j, \tag{18}$$

with $|z| > 1$ corresponding to an unstable mode. κ_q and κ_r are necessarily related to z through the interior equations which require that

$$z = 1 - \lambda(1 - \kappa_q^{-1}), \qquad z = 1 + \lambda(\kappa_r - 1). \tag{19}$$

λ is the CFL parameter $c\Delta t/\Delta x$ and must satisfy the Fourier stability restriction $\lambda \leqslant 1$. It can be shown that if $|z| > 1$, then $|\kappa_q| < 1$ and $|\kappa_r| > 1$. Hence, to satisfy the discrete equivalent of the radiation condition that all variables tend to zero as $j \to \infty$, it is necessary that $R = 0$.

3.1.1. Explicit first-order coupling. The final discrete equation is the kinematic compatibility condition. A simple first order approximation of this is

$$\frac{1}{\Delta t}(x_{\mathrm{w}}^{(n+1)} - x_{\mathrm{w}}^{(n)}) = \frac{1}{2\rho c}(q_0^{(n+1)} - r_0^{(n+1)}). \tag{20}$$

Inserting the assumed G–R mode into the wall dynamic equation and this kinematic equation yields the two equations

$$\left(\frac{m}{\Delta t^2}(z - 2 + z^{-1}) + m\omega_0^2\right)X = -\tfrac{1}{2}Q, \qquad \frac{z-1}{\Delta t}X = \frac{z}{2\rho c}Q, \tag{21}$$

for which there are non-trivial solutions only if

$$z - 2 + z^{-1} + (\omega_0\Delta t)^2 = -2d\omega_0\Delta t(1 - z^{-1}), \tag{22}$$

where d is still the non-dimensional damping factor $d = \rho c/2m\omega_0$. Multiplying by z produces a quadratic equation. When $d = 0$, the roots of this are

$$z = 1 - \tfrac{1}{2}(\omega_0\Delta t)^2 \pm \mathrm{i}\omega_0\Delta t\sqrt{[1 - \tfrac{1}{4}(\omega_0\Delta t)^2]}. \tag{23}$$

If $\omega_0\Delta t \leqslant 2$, then the two roots are a complex conjugate pair of unit magnitude, while if $\omega_0\Delta t > 2$ then the two roots are real and negative, with one having a magnitude greater than unity, giving unstable exponential growth. Thus, numerical stability in the absence of any aerodynamic coupling requires $\omega_0\Delta t \leqslant 2$. This means that there must be more than three time steps per period of oscillation, but it is clear that many more time steps than this are required for accuracy and so this stability criterion is not significant.

When $0 < d < 1$, we look for roots of the quadratic for which $|z| = 1$, corresponding to the threshold of instability.

Considering first the case in which the roots form a complex conjugate pair, from the coefficients of the quadratic equation, the product of the roots is $1 - d\omega_0\Delta t$. Hence, if $\omega_0\Delta t \leqslant 2$, then the two roots have magnitude less than unity.

Considering next the case in which both roots of the quadratic are real, $z = 1$ is never a solution for $\Delta t > 0$ and $z = -1$ is a solution only when

$$4 - (\omega_0\Delta t)^2 - 2d(\omega_0\Delta t) = 0. \tag{24}$$

Thus the stability limit of the coupled problem is

$$\omega_0\Delta t \leqslant \sqrt{(4 + d^2)} - d < 2. \tag{25}$$

Assuming there are sufficient time steps per period to achieve an accurate solution, there is therefore no numerical stability problem.

To determine the accuracy we let $z = e^{i\omega\Delta t}$, which gives

$$e^{i\omega\Delta t} - 2 + e^{-i\omega\Delta t} + (\omega_0\Delta t)^2 = -2d\omega_0\Delta t(1 - e^{-i\omega\Delta t}). \tag{26}$$

Performing a Taylor series expansion in both d and $\omega_0\Delta t$ yields

$$\frac{\omega}{\omega_0} \approx 1 + id - \tfrac{1}{2}d^2 + \tfrac{1}{2}d\omega_0\Delta t + id^2\omega_0\Delta t + \tfrac{1}{24}(\omega_0\Delta t)^2 + O(d^4, (\omega_0\Delta t)^4). \tag{27}$$

This shows that the first order error in the coupling produces a first order error in both the real and imaginary components of the complex frequency, corresponding to the frequency and damping rate of the coupled oscillation respectively.

The accuracy of this analysis is shown in Figure 2. Numerical calculations were performed for $\omega_0\Delta t = 0.02, 0.05, 0.1$ and 0.2 (corresponding approximately to 300, 120, 60 and 30 time steps per period) and values of d in the range 0.005–0.1. Each calculation was performed for 10,000 iterations and from the results the frequency and damping rate were deduced. These are presented as full lines in the two parts of Figure 2, while the broken lines show the predictions from the asymptotic analysis above. The agreement is excellent over the whole parameter range studied.
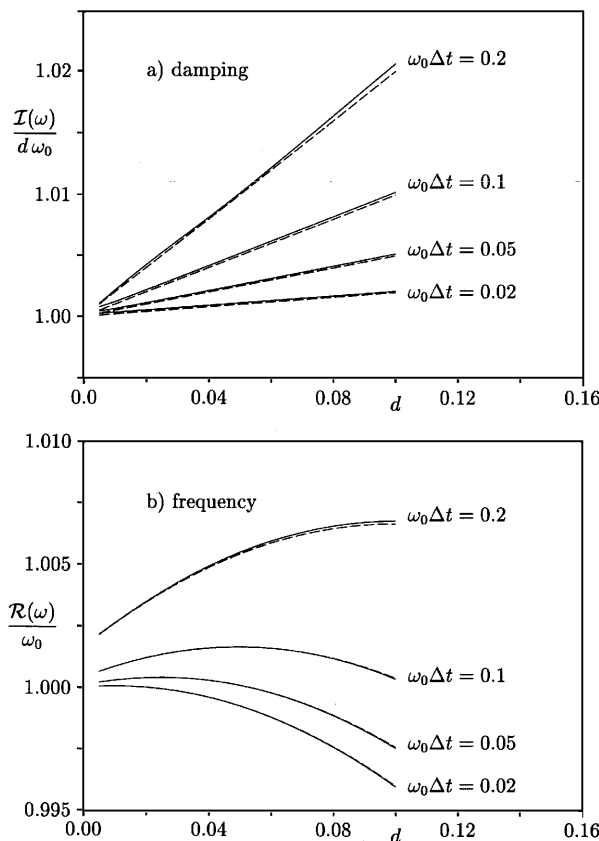

Figure 2. Damping and frequency using explicit first-order coupling method (full lines, numerical computation; broken lines, numerical analysis)

For a typical flutter frequency and a time step limited by the CFL stability restriction $c\Delta t/\Delta x < 1$ for a typical grid resolution, $\omega_0 \Delta t$ will be in the range 10^{-3}–10^{-2}. In this case the errors in both the frequency and damping are negligible compared with other errors such as modelling approximations and uncertainty about structural damping factors.

This conclusion about the adequacy of first order coupling changes entirely when one considers implicit methods. Replacing the forward time differencing of the aerodynamics by backward time differencing gives the following algorithm for the aerodynamics.

$$
q_j^{(n+1)} = q_j^{(n)} - \frac{c\Delta t}{\Delta x}(q_j^{(n+1)} - q_{j-1}^{(n+1)}), \quad j = 0, 1, 2, \ldots,
$$

$$
r_j^{(n+1)} = r_j^{(n)} + \frac{c\Delta t}{\Delta x}(r_{j+1}^{(n+1)} - r_j^{(n+1)}), \quad j = 0, 1, 2, \ldots.
$$
(28)

All the previous analysis remains valid. This surprising fact is because the wall coupling equations do not depend on the interior equations once it is determined that $r_j^{(n)}$ is zero throughout the domain in order to satisfy the discrete radiation condition. The conclusions about the accuracy change because the time step is no longer limited by the CFL condition. Instead, $\omega_0 \Delta t$ will typically be $O(10^{-1})$. It is the computational efficiency of this much larger time step which is the attraction of using implicit methods for flutter analysis and other unsteady flow calculations at low reduced frequencies.[9,10] However, as a consequence the first order coupling is no longer sufficiently accurate.

3.1.2. An explicit second-order coupling. A second-order accurate coupling is achieved by changing the kinematic discretization to

$$
\frac{1}{\Delta t}(\tfrac{3}{2}x_w^{(n+1)} - 2x_w^{(n)} + \tfrac{1}{2}x_w^{(n-1)}) = \frac{1}{2\rho c}(q_0^{(n+1)} - r_0^{(n+1)}),
$$
(29)

which leads to the following modified equation for z:

$$
z - 2 + z^{-1} + (\omega_0 \Delta t)^2 = -2d\omega_0 \Delta t (\tfrac{3}{2} - 2z^{-1} + \tfrac{1}{2}z^{-2}).
$$
(30)

Multiplying by z^2 now gives a cubic equation in z. In the limit as $d \to 0$ two of the roots are the same as before and the third is $z = 0$. This third root is only slightly perturbed when $0 < d \ll 1$ and so remains strongly stable. To find the perturbation to the other two roots it is convenient again to make the substitution $z = e^{i\omega\Delta t}$, giving

$$
e^{i\omega\Delta t} - 2 + e^{-i\omega\Delta t} + (\omega_0 \Delta t)^2 = -2d\omega_0 \Delta t (\tfrac{3}{2} - 2e^{-i\omega\Delta t} + \tfrac{1}{2}e^{-2i\omega\Delta t}).
$$
(31)

Differentiating with respect to d gives

$$
\frac{\partial \omega}{\partial d} = \omega_0 \left[i + 2i \sin^2\left(\frac{\omega\Delta t}{2}\right) + 2\tan\left(\frac{\omega\Delta t}{2}\right)\sin^2\left(\frac{\omega\Delta t}{2}\right) \right].
$$
(32)

The two roots which are neutrally stable when $d = 0$ and $\omega_0 \Delta t < 2$ have corresponding real values for ω. The imaginary part of $\partial \omega/\partial d$ is then positive, showing that the perturbed roots are stable. The stability boundary for $0 < d \ll 1$ therefore remains $\omega_0 \Delta t < 2$.

A Taylor series expansion of equation (31) yields

$$
\frac{\omega}{\omega_0} \approx 1 + id - \tfrac{1}{2}d^2 + \tfrac{1}{24}(\omega_0 \Delta t)^2 + \tfrac{1}{2}id(\omega_0 \Delta t)^2 + O(d^4, (\omega_0 \Delta t)^4).
$$
(33)

Because of the improved accuracy of the kinematic discretization the error is now second order in $\omega_0 \Delta t$. If $\omega_0 \Delta t = 0 \cdot 1$, corresponding to approximately 60 time steps per period, then the error is probably acceptable; if $\omega_0 \Delta t = 0 \cdot 3$, corresponding to approximately 20 time steps per period, then
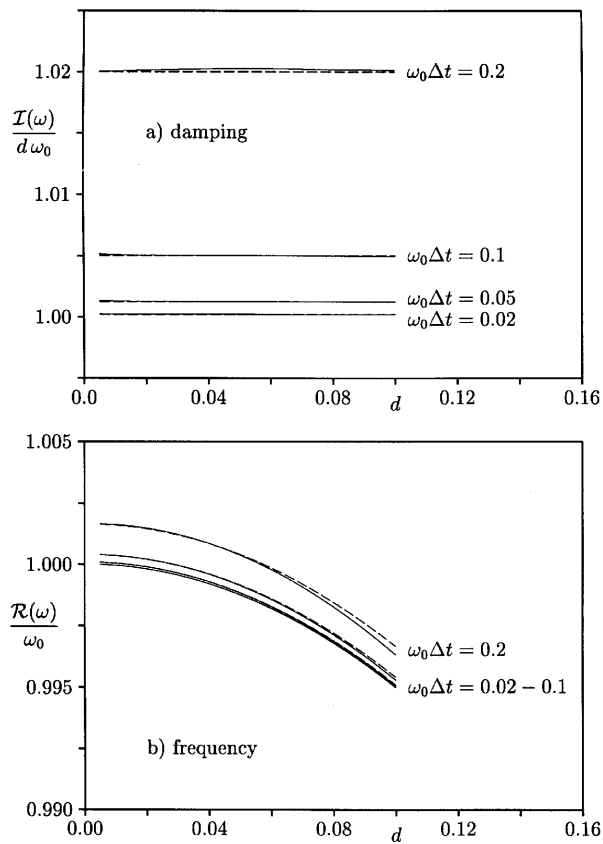
Figure 3. Damping and frequency using explicit second-order coupling method (full lines, numerical computation; broken lines, numerical analysis)

the error is probably unacceptable. The accuracy of this asymptotic analysis is shown by the numerical results in Figure 3.

3.1.3. An unstable second-order coupling. Another second-order accurate discretization of the kinematic condition is

$$\frac{1}{\Delta t}(x_w^{(n+1)} - x_w^{(n)}) = \frac{1}{4\rho c}(q_0^{(n)} + q_0^{(n+1)} - r_0^{(n)} - r_0^{(n+1)}), \tag{34}$$

which leads to the following modified equation for z:

$$z - 2 + z^{-1} + (\omega_0\Delta t)^2 = -4d\omega_0\Delta t \frac{z-1}{z+1}. \tag{35}$$

Multiplying by $z + 1$ gives a cubic equation in z. The product of its three roots is -1, and so the only possibility for stability is if one root is -1 and the other two form a complex comjugate pair of unit magnitude. However, $z = -1$ is not a root if d is non-zero, and therefore the coupled system is unconditionally unstable.

Asymptotic analysis shows that the unstable root is

$$z = -1 - 2d\omega_0\Delta t + O(d^2(\omega_0\Delta t)^2), \tag{36}$$

corresponding to a saw-tooth oscillation in time with a slowly growing amplitude. This is confirmed by the numerical results in Figure 4 for $d = 0\cdot1$ and $\omega_0\Delta t = 0\cdot2$.

3.1.4. An implicit second-order coupling. Yet another second-order-accurate discretization is

$$\frac{1}{2\Delta t}(x_w^{(n+1)} - x_w^{(n-1)}) = \frac{1}{2\rho c}(q_0^{(n)} - r_0^{(n)}), \tag{37}$$

which leads to the following modified equation for z:

$$z - 2 + z^{-1} + (\omega_0\Delta t)^2 = -d\omega_0\Delta t(z - z^{-1}). \tag{38}$$

Multiplying by z gives a quadratic equation with no spurious roots. Substituting $z = e^{i\omega\Delta t}$ and differentiating yields

$$\frac{\partial \omega}{\partial d} = i\omega_0 \tag{39}$$

and so the perturbed roots are stable for $\omega_0\Delta t < 2$ and $0 < d \ll 1$.

Asymptotic analysis yields

$$\frac{\omega}{\omega_0} \approx 1 + id - \tfrac{1}{2}d^2 + \tfrac{1}{24}(\omega_0\Delta t)^2 + O(d^4, d(\omega_0\Delta t)^2, (\omega_0\Delta t)^4). \tag{40}$$

The problem with this kinematic discretization is that it is now an implicit algorithm since the surface pressure $p_0^{(n)}$ depends on $x_w^{(n+1)}$, and *vice versa*. This implicitness is awkward because in a 3D application it means that the aerodynamic variables at all grid points on the surface of the vibrating
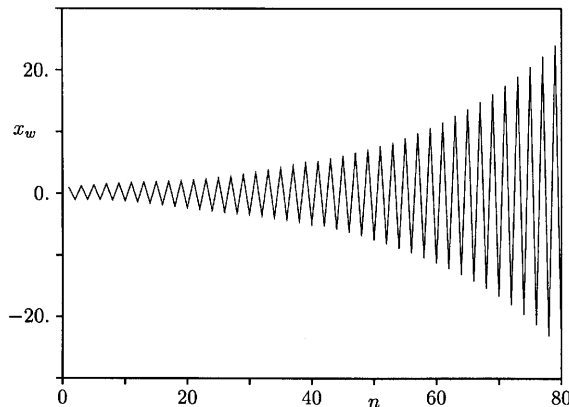

Figure 4. Numerical computation using unstable second-order coupling method

blade are coupled through the structural boundary conditions. The difficulty can be overcome by a predictor/corrector implementation:

$$\frac{m}{\Delta t^2}(x_w^* - 2x_w^{(n)} + x_w^{(n-1)}) + m\omega_0^2 x_w^{(n)} = -p_0^{(n-1)} \quad \Big\} \quad \text{predictor,}$$

$$p_0^{(n)} = p_0^{(n)}(x_w^{(n-1)}, x_w^{(n)}, x_w^*, q_j^{(n-1)}, r_j^{(n-1)})$$

$$\frac{m}{\Delta t^2}(x_w^{(n+1)} - 2x_w^{(n)} + x_w^{(n-1)}) + m\omega_0^2 x_w^{(n)} = -p_0^{(n)} \quad \Bigg\} \quad \text{corrector.}$$

$$\tag{41}$$

In the prediction stage a first approximation for the surface pressure $p_0^{(n)}$ is given by the pressure $p_0^{(n-1)}$ at the previous time step, and this is used to obtain a first estimate for $x_w^{(n+1)}$. In the correction stage the predicted value x_w^* is used in conjunction with the discrete aerodynamic equations and kinematic boundary condition to calculate a corrected value for $p_0^{(n)}$; this is then used to calculate a corrected value for $x_w^{(n+1)}$.

The error introduced by this predictor/corrector approximation to the original implicit algorithm is $O((d\omega_0\Delta t)^2)$, and so the asymptotic expression for the complex frequency in equation (40) remains valid. This is confirmed by Figure 5 which shows the frequency and decay rates of the results
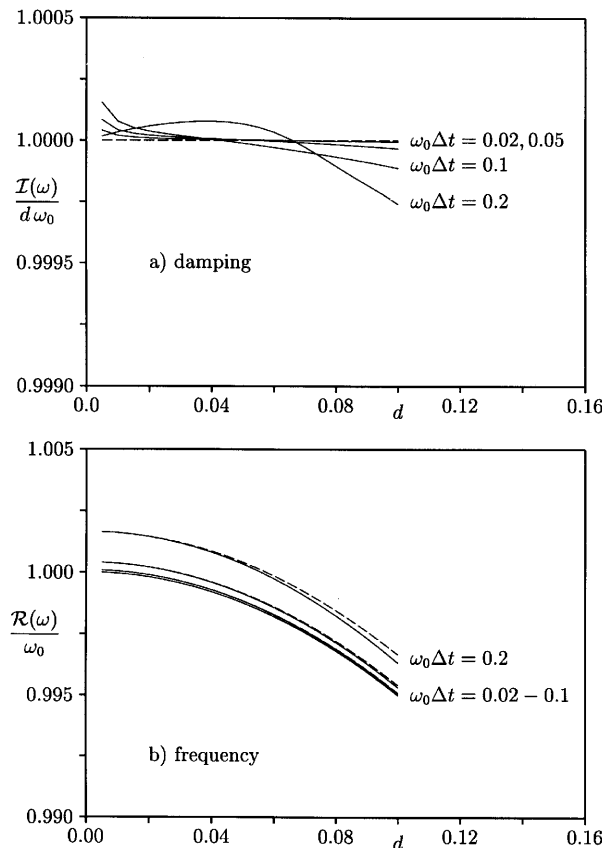

Figure 5. Damping and frequency using second-order predictor/corrector method (full lines, numerical computation; broken lines, numerical analysis)

obtained using the predictor/corrector method. There is excellent agreement with the predictions of the asymptotic analysis.

4. STRUCTURAL ALGORITHMS BASED ON WALL DISPLACEMENT AND VELOCITY

In this section we consider coupled aeroelastic discretizations based on the vector form of the wall dynamic equation. An advantage of this approach is that by calculating both the displacement and velocity at each time step, the kinematic boundary condition becomes simply

$$\dot{x}_{\text{w}}^{(n)} = u_0^{(n)}. \tag{42}$$

4.1. Trapezoidal integration

The simplest second-order-accurate discretization of the vector form of the wall dynamic equation is trapezoidal integration (also known as the Crank–Nicolson or *box* method):

$$\frac{1}{\Delta t}(w^{(n+1)} - w^{(n)}) + \tfrac{1}{2}A(w^{(n+1)} + w^{(n)}) = \tfrac{1}{2}(P^{(n+1)} + P^{(n)}). \tag{43}$$

Assuming that upwind differencing is used for the aerodynamic equations then $r_j^{(n)} = 0$ for all j and n, and hence

$$P^{(n)} = \begin{pmatrix} 0 \\ -(\rho c/m)\dot{x}_{\text{w}}^{(n)} \end{pmatrix} = \begin{pmatrix} 0 \\ -2d\omega_0\dot{x}_{\text{w}}^{(n)} \end{pmatrix}. \tag{44}$$

Therefore equation (43) becomes

$$\begin{pmatrix} 1 & -\tfrac{1}{2}\omega_0\Delta t \\ \tfrac{1}{2}\omega_0\Delta t & 1 + d\omega_0\Delta t \end{pmatrix}w^{(n+1)} = \begin{pmatrix} 1 & \tfrac{1}{2}\omega_0\Delta t \\ -\tfrac{1}{2}\omega_0\Delta t & 1 - d\omega_0\Delta t \end{pmatrix}w^{(n)}. \tag{45}$$

$w^{(n)} = z^n W$ is a solution for some non-trivial constant vector W if and only if,

$$\det\begin{pmatrix} z - 1 & -\tfrac{1}{2}\omega_0\Delta t(z + 1) \\ \tfrac{1}{2}\omega_0\Delta t(z + 1) & z - 1 + d\omega_0\Delta t(z + 1) \end{pmatrix} = 0$$

$$\Rightarrow \quad z^2\left[1 + \left(\frac{\omega_0\Delta t}{2}\right)^2 + d\omega_0\Delta t\right] - 2z\left[1 - \left(\frac{\omega_0\Delta t}{2}\right)^2\right] + \left[1 + \left(\frac{\omega_0\Delta t}{2}\right)^2 - d\omega_0\Delta t\right] = 0$$

$$\Rightarrow \quad z = \frac{1 - (\omega_0\Delta t/2)^2 \pm \mathrm{i}\omega_0\Delta t\sqrt{(1 - d^2)}}{1 + (\omega_0\Delta t/2)^2 + d\omega_0\Delta t}. \tag{46}$$

Provided that $0 < d < 1$, the two roots form a complex conjugate pair with magnitude less than unity. Therefore the coupled algorithm is unconditionally stable. In addition, setting $z = \exp(\pm \mathrm{i}\omega\Delta t)$, and performing a Taylor series expansion yields

$$\frac{\omega}{\omega_0} = 1 + \mathrm{i}d - \tfrac{1}{2}d^2 - \tfrac{1}{12}(\omega_0\Delta t)^2 - \tfrac{1}{4}\mathrm{i}d(\omega_0\Delta t)^2 + O(d^4, (\omega_0\Delta t)^4). \tag{47}$$

As with the implicit method of the last section, there is the problem that $w^{(n+1)}$ depends on $P^{(n+1)}$, and *vice versa*. This is again solved using a predictor/corrector procedure:

$$w^* = (I + \tfrac{1}{2}\Delta tA)^{-1}[(I - \tfrac{1}{2}\Delta tA)w^{(n)} + \Delta tP^{(n)}] \qquad \} \quad \text{predictor,}$$

$$P^{(n+1)} = P^{(n+1)}(w^{(n)}, w^*, q_j^{(n)}, r_j^{(n)})$$

$$w^{(n+1)} = (I + \tfrac{1}{2}\Delta tA)^{-1}[(I - \tfrac{1}{2}\Delta tA)w^{(n)} + \tfrac{1}{2}\Delta t(P^{(n+1)} + P^{(n)})] \qquad \Bigg\} \quad \text{corrector.} \qquad (48)$$

As before, the predictor/corrector combination gives results which are within $O((d\omega_0\Delta t)^2)$ of those which would be obtained from the original implicit coupling. This is confirmed by Figure 6 which shows the results obtained using this predictor/corrector variant of the trapezoidal algorithm. Provided that $\omega_0\Delta t < 0.2$, corresponding to there being at least 30 time steps per period, the frequency and damping are both correct to within 1%, which is perfectly acceptable accuracy for engineering purposes..
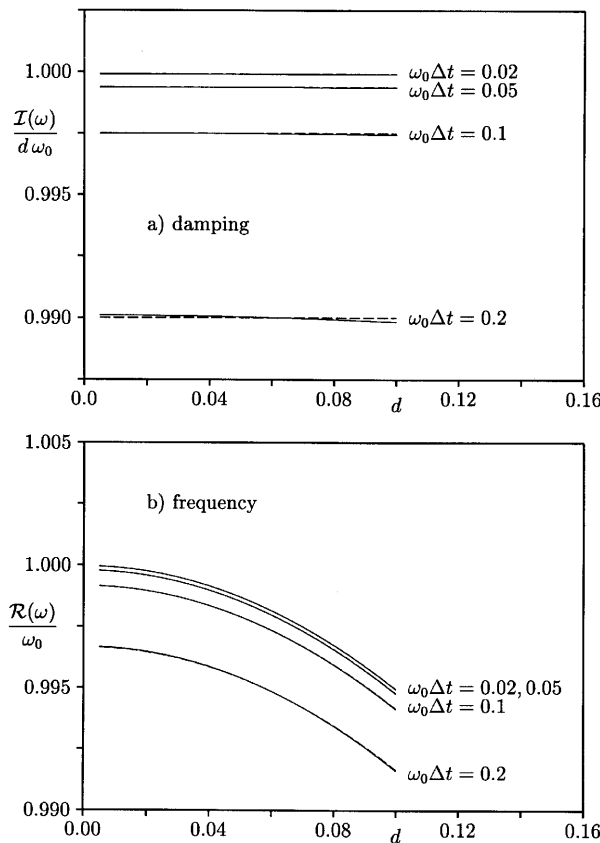

Figure 6. Damping and frequency using second-order trapezoidal method (full lines, numerical computation; broken lines, numerical analysis)

4.2. Second-order backward differentiation

Another second order accurate approximation of the dynamic equation is

$$\frac{1}{\Delta t}(\tfrac{3}{2}w^{(n+1)} - 2w^{(n)} + \tfrac{1}{2}w^{(n-1)}) + Aw^{(n+1)} = P^{(n+1)}. \tag{49}$$

This is the method used by Alonso *et al.*[11] for aeroelastic computations in which the fluid is water and so the corresponding value for d is much larger than for aeronautical applications. As with the last method, it can be implemented using a predictor/corrector procedure to avoid the complications of an implicit algorithm. Alonso *et al.* use several correction stages within a time-accurate multigrid procedure because of the much larger effect of the fluid dynamics on the structural behaviour.[11]

The determinant condition for this discretization is

$$\det\begin{pmatrix} \tfrac{3}{2}z - 2 - \tfrac{1}{2}z^{-1} & -z\omega_0\Delta t \\ z\omega_0\Delta t & \tfrac{3}{2}z - 2 - \tfrac{1}{2}z^{-1} + 2zd\omega_0\Delta t \end{pmatrix} = 0$$

$$\Rightarrow \quad (\tfrac{3}{2} - 2z^{-1} + \tfrac{1}{2}z^{-2})^2 + 2d\omega_0\Delta t(\tfrac{3}{2} - 2z^{-1} + \tfrac{1}{2}z^{-2}) + (\omega_0\Delta t)^2 = 0. \tag{50}$$

When $d = 0$, this reduces to

$$\tfrac{3}{2} - 2z^{-1} + \tfrac{1}{2}z^{-2} = \mathrm{i}\omega_0\Delta t. \tag{51}$$

It can be shown that both roots have less than unit magnitude for all values of $\omega_0\Delta t$. In particular, when $\omega_0\Delta t \ll 1$, one root is a strongly stable spurious root ($z \approx \tfrac{1}{3}$). The other root can be expressed as $z = \exp(\mathrm{i}\omega\Delta t)$ for which asymptotic analysis gives

$$\frac{\omega}{\omega_0} \approx 1 - \tfrac{1}{3}(\omega_0\Delta t)^2 + \tfrac{1}{4}\mathrm{i}(\omega_0\Delta t)^3, \tag{52}$$

showing that there is third-order numerical damping of the wall oscillation in the absence of any aerodynamic damping.

When $0 < d < 1$, asymptotic analysis yields

$$\frac{\omega}{\omega_0} = 1 + \mathrm{i}d - \tfrac{1}{2}d^2 - \tfrac{1}{3}(\omega_0\Delta t)^2 - \mathrm{i}d(\omega_0\Delta t)^2 + \tfrac{1}{4}\mathrm{i}(\omega_0\Delta t)^3 + O(d^4, (\omega_0\Delta t)^4). \tag{53}$$

Figure 7 presents these asymptotic predictions along with numerical results using a predictor/corrector implementation of the algorithm. The results confirm that this method is significantly less accurate than the method based on trapezoidal integration. The error in the real part of the frequency and one of the errors in the damping are both four times greater. Also, this algorithm gives numerical damping of the uncoupled wall dynamics; this numerical damping of magnitude $\tfrac{1}{4}(\omega_0\Delta t)^3$ is significant relative to the true physical damping when d is 0·005–0·02 and $\omega_0\Delta t$ is 0·1 or larger.

This same criticism can be applied to many other methods frequently used for structural dynamics, including the Houboult, Wilson-θ and Newmark-β methods and the multiparameter unified schemes of Zienkiewicz *et al.*[12] and Thomas and Gladwell.[13] Some of these methods always introduce numerical damping; the others depend on a set of parameters which are often chosen to ensure some level of numerical damping. The reason that structural dynamicists prefer methods with numerical damping is that they are usually integrating very large stiff systems of equations in which some very high frequency modes are not adequately resolved by the chosen time step. Therefore (quoting from the paper by Thomas and Gladwell[13]) 'in practice we use methods which are damped ... since this ensures that the highly oscillatory eigenfunctions ... excited by noise in the initial data are damped out quickly'.
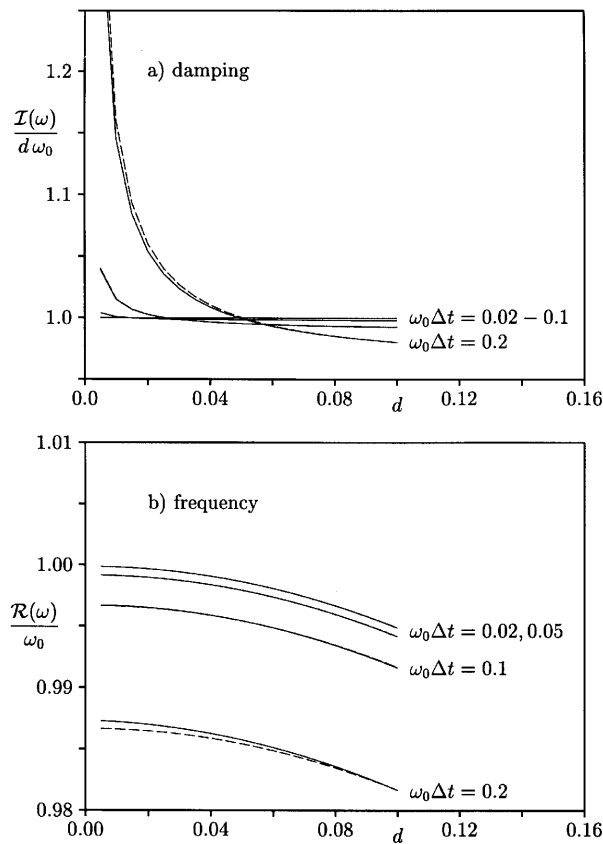
Figure 7. Damping and frequency using backward differencing method (full lines, numerical computation; broken lines, numerical analysis)

In the application in this paper there is only one structural eigenmode and so this concern does not arise. Furthermore, in a real 3D application it is assumed that a reduced modal representation of the structural dynamics would be used,[1-3,14] perhaps using the lowest five eigenmodes, and so again there would be no problem of numerical stiffness. If a very large number of structural igenmodes are retained it may become desirable in implicit calculations to introduce structural damping into the equations for the highest frequency modes only, since these frequencies are unlikely to be adequately resolved by the large time step.

4.3. State-transition algorithm

The state transition algorithm[10,15] is an alternative approximation of the vector version of the wall dynamics equation. The algorithm is designed to be exact when there is no aerodynamic coupling. The exponential matrix $\exp(tA)$ is defined for an arbitrary matrix A as

$$\exp(tA) = \sum_0^\infty \frac{t^n}{n!} A^n. \tag{54}$$

By definition, A^0 is the identity matrix I and so $\exp(tA) = I$ when $t = 0$. Another important property of the exponential matrix is that

$$\frac{\mathrm{d}}{\mathrm{d}t}\exp(tA) = \exp(tA)A. \tag{55}$$

For the particular matrix A in this analysis,

$$\exp(tA) = \begin{pmatrix} \cos(\omega_0 t) & -(\omega_0 t) \\ \sin(\omega_0 t) & \cos(\omega_0 t) \end{pmatrix}. \tag{56}$$

This can be verified by checking that it satisfies the above two conditions or by directly evaluating A^n and using the series expansions for $\cos(\omega_0 t)$ and $\sin(\omega_0 t)$. Using this matrix, it follows immediately that

$$\frac{\mathrm{d}}{\mathrm{d}t}[\exp(tA)w] = \exp(tA)\frac{\mathrm{d}w}{\mathrm{d}t} + \exp(tA)Aw = \exp(tA)P \tag{57}$$

and hence

$$w(t_0) - \exp(-t_0 A)\,w(0) = \int_0^{t_0} \exp[(t - t_0)A]\,P(t)\mathrm{d}t. \tag{58}$$

The state transition method uses this equation with $t_0 = \Delta t$ and a suitable approximation to the integral. The approximation used by Edwards et al.[15] is

$$\int_0^{t_0} \exp[(t - t_0)A]P(t)\mathrm{d}t \approx \left(\int_0^{t_0} \exp[(t - t_0)A]\mathrm{d}t \right)\tfrac{1}{2}[P(0) + P(t_0)]. \tag{59}$$

Since

$$\int_0^{t_0} \exp[(t - t_0)A]\mathrm{d}t = A^{-1}[I - \exp(-t_0 A)], \tag{60}$$

the resulting algorithm is

$$w^{(n+1)} = \exp(-\Delta t A)w^{(n)} + \tfrac{1}{2}A^{-1}[I - \exp(-\Delta t A)](P^{(n)} + P^{(n+1)}). \tag{61}$$

The determinant condition for the eigenvalue z leads to a quadratic equation,

$$z^2[1 + d\sin(\omega_0\Delta t)] - 2z\cos(\omega_0\Delta t) + [1 - d\sin(\omega_0\Delta t)] = 0$$

$$\Rightarrow \quad z = \frac{\cos(\omega_0\Delta t) \pm \mathrm{i}\sin(\omega_0\Delta t)\sqrt{(1 - d^2)}}{1 + d\sin(\omega_0\Delta t)}. \tag{62}$$

When $0 < d < 1$, the two roots form a complex conjugate pair whose magnitude is less than unity provided that $\sin(\omega\Delta t) > 0$; this condition is satisifed if there are more than two time steps per period of oscillation.

Asymptotic analysis leads to

$$\frac{\omega}{\omega_0} = 1 + \mathrm{i}d - \tfrac{1}{2}d^2 + \tfrac{1}{6}\mathrm{i}d(\omega_0\Delta t)^2 + O(d^4, (\omega_0\Delta t)^4). \tag{63}$$

Numerical results using a predictor/corrector implementation are shown in Figure 8. As predicted, the frequency is determined very accurately even when using very few time steps per period, but there is a second order error in the damping.
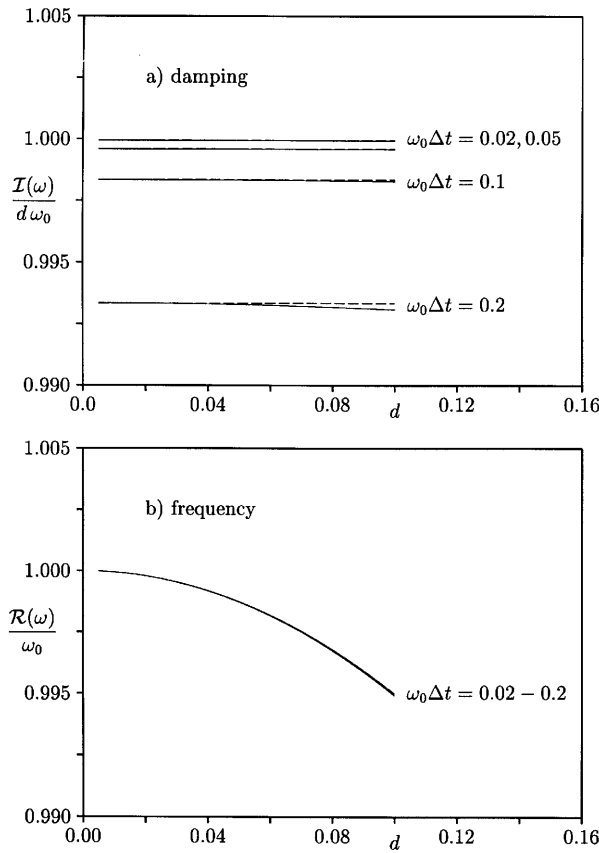
Figure 8. Damping and frequency using first variant of state transition method (full lines, numerical computation; broken lines, numerical analysis)

An improved variant of the state transition algorithm is obtained by approximating the pressure integral as

$$\int_0^{t_0} \exp[(t - t_0)A]P(t)\mathrm{d}t \approx \frac{t_0}{2}[\exp(-t_0 A)P(0) + P(t_0)], \qquad (64)$$

giving the algorithm

$$w^{(n+1)} = \exp(-\Delta t A)(w^{(n)} + \tfrac{1}{2}\Delta t P^{(n)}) + \tfrac{1}{2}\Delta t P^{(n+1)}. \qquad (65)$$

The determinant condition leads to

$$z^2(1 + d\omega_0\Delta t) - 2z\cos(\omega_0\Delta t) + (1 - d\omega_0\Delta t) = 0$$

$$\Rightarrow \quad z = \frac{\cos(\omega_0\Delta t) \pm \sqrt{[-\sin^2(\omega_0\Delta t) + (d\omega_0\Delta t)^2]}}{1 + d\omega_0\Delta t}. \qquad (66)$$
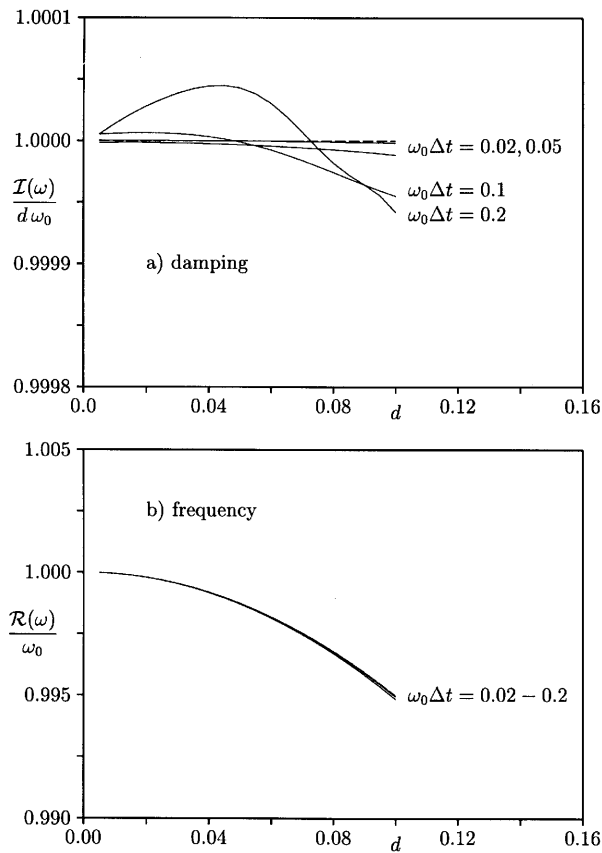
Figure 9. Damping and frequency using second variant of state transition method (full lines, numerical computation; broken lines, numerical analysis)

The two roots are stable for all values of d and $\omega_0\Delta t$. Asymptotic analysis yields

$$\frac{\omega}{\omega_0} = 1 + id - \tfrac{1}{2}d^2 + O(d^4, (\omega_0\Delta t)^4), \tag{67}$$

which means that, to within the accuracy of the asymptotic analysis, the numerical results should perfectly match the analytic behaviour. This prediction is verified by the results shown in Figure 9, which as usual are obtained using a predictor/corrector implementation.

5. DISCUSSION OF RELEVANCE TO 3D APPLICATIONS

The interpretation of the analysis in this paper in the context of real 3D engineering calculations is a tricky issue. The simple model problem in the current analysis has a one-degree-of-freedom structural oscillation in which the surface pressure varies in phase with the wall velocity, causing aerodynamic damping under all conditions. In a real application the structural model will have several degrees of freedom. For each degree of freedom there is a corresponding *generalised force* which is the combined effect of the entire surface pressure distribution on the particular mode of vibration. The non-dimensional generalized force will have magnitude corresponding to the damping factor d in the model problem, but unlike in the model problem the generalized force will not be perfectly in phase

with the mode motion. Flutter, a physical instability of the coupled aeroelastic system, occurs when the phase difference between the force and the velocity of the mode is less than $90°$. This corresponds to redefining the damping factor d in the model analysis to be a complex quantity with negative real component. For accurate prediction of the conditions under which flutter occurs, it is therefore the phase rather than the magnitude of the aerodynamics which must be accurately represented by the numerical discretization. Treating d as a general complex quantity, it can be seen that the first order coupling leads to significant phase errors unless the time step is very small. The analysis of the second order coupling shows that the leading error is in the magnitude of the aerodynamic effect; there is only a third-order error in its phase. These methods are therefore very much more accurate.

6. CONCLUSIONS

By performing a detailed analysis of a relatively simple 1D model problem, this paper has tried to address the issues of stability and accuracy in the discretization of aeroelastic systems. The key non-dimensional physical parameter in the model problem is the aerodynamic damping factor d. The corresponding parameter in turbomachinery applications lies in the range 0·005–0·02 while for aircraft applications it is usually in the range 0·05–0·2.

There appears to be no possibility of a spurious numerical instability due to the coupling of the aerodynamic and structural models, provided that there are no unstable or neutrally stable spurious modes in the uncoupled limit as $d \to 0$. The numerical accuracy has been assessed by asymptotic analysis of the complex frequency obtained from the coupled discretizations. Numerical experiments demonstrate the accuracy of the asymptotic analysis when there are at least 30 time steps per period and the damping is in the range 0·005–0·1.

If an explicit CFD algorithm is used for the aerodynamic equations, then for typical flutter frequencies and aerodynamic grid resolution the number of time steps per period will be $O(10^3)$. Hence any stable algorithm for the discretization of the structural dynamics and the kinematic boundary condition will be sufficiently accurate provided that it is at least second order accurate for the uncoupled vibration, and first order accurate for the coupled analysis.

If, on the other hand, an implicit CFD algorithm is used for the aerodynamic equations, then it is possible that there may be as few as 30 time steps per period. In this case it is necessary to use a discretization which is second-order accurate for both the uncoupled and coupled systems. Almost any of the second order methods analysed in this paper could be used with confidence; in real 3D computations the errors due to the unsteady flow discretization will probably be much greater than those due to the aeroelastic coupling algorithm. However, for turbomachinery applications with extremely low levels of physical damping it is best to avoid the use of the many standard algorithms which cause spurious numerical damping of the uncoupled wall dynamics.

REFERENCES

1. G. P. Guruswamy, 'ENSAERO—a multidisciplinary program for fluid/structural interaction studies of aerospace vehicles', *Comput. Syst. Eng.*, **1**, 237–256 (1990).
2. G. P. Guruswamy, 'Unsteady aerodynamic and aeroelastic calculations for wings under Euler equations', *AIAA J.*, **28**, (1990).

3. J. G. Marshall and M. Imregun, 'A 3D time-domain flutter prediction method for turbomachinery blades', *Proc. Int. Forum on Aeroelasticity and Structural Dynamics*, Royal Aeronautical Society, Manchester, 1995.
4. T. Nomura and T. J. R. Hughes, 'An arbitrary Lagrangian–Eulerian finite element method for interaction of fluid and a rigid body', *Comput. Methods Appl. Mech. Eng.*, **95**, 115–138 (1992).
5. S. K. Godunov and V. S. Ryabenkii, *The Theory of Difference Schemes—An Introduction*, North-Holland, Amsterdam, 1964.
6. B. Gustafsson, H.-O. Kreiss and A. Sundström, 'Stability theory of difference approximations for mixed initial boundary value problems. II', *Math. Comput.*, **26**, 649–686 (1972).
7. R. D. Richtmyer and K. W. Morton, *Difference Methods for Initial Value Problems*, Wiley–Interscience, 2nd edn, 1967.
8. L. N. Trefethen, 'Group velocity interpretation of the stability theory of Gustafsson, Kreiss, and Sundström, *J. Comput. Phys.*, **49**, 199–217 (1983).
9. A. Jameson, 'Time dependent calculations using multigrid with applications to unsteady flows past airfoils, wings and rotors', *AIAA Paper 91-1596*, 1991.
10. R. D. Rausch, J. T., Batina and H. T. Y. Yang, 'Three-dimensional time-marching aeroelastic analyses using an unstructured-grid Euler method', *AIAα J.*, **31**, 1626–1633 (1993).
11. J. Alonso, L. Martinelli and A. Jameson, 'Multigrid unsteady Navier–Stokes calculations with aeroelastic applications', *AIAA Paper 95-0048*, 1995.
12. O.Zienkiewicz, W. Wood, N. Hine and R. Taylor, 'U unified set of single step algorithms. Part I: General formulation and applications', *Int. j. numer. methods eng.*, **20**, **20**, 1529–1552 (1984).
13. R. Thomas and I. Gladwell, 'Variable-order variable-step algorithms for second-order systems. Part I: The methods', *Int. j. numer. methods eng.*, **26**, 39–53 (1988).
14. B Winzell, 'Recent applications of linear and nonlinear unsteady aerodynamics for aeroelastic analysis', *AGARD CP 506*, 1991.
15. J. W. Edwards, R. M. Bennett, W. Whitlow and D. A. Seidel, 'Time-marching transonic flutter solutions including angle-of-attack effects', *J. Aircraft*, **20**, 899–906 (1983).